analytical chemistry

Article

Cite This: Anal. Chem. 2018, 90, 10279−10285

pubs.acs.org/ac

Nonfouling, Encoded Hydrogel Microparticles for Multiplex MicroRNA Profiling Directly from Formalin-Fixed, Paraffin-Embedded Tissue

Maxwell B. Nagarajan,[†] Augusto M. Tentori,[†] Wen Cai Zhang,[‡] Frank J. Slack,[‡] and Patrick S. Doyle*[,†]

[†]Department of Chemical Engineering, Massachusetts Institute of Technology, Cambridge, Massachusetts 02139, United States

[‡]HMS Initiative for RNA Medicine, Department of Pathology, Beth Israel Deaconess Medical Center, Harvard Medical School, 330 Brookline Avenue, Boston, Massachusetts 02215, United States

Supporting Information

ABSTRACT: MicroRNAs (miRNA) are short, noncoding RNAs that have been implicated in many diseases, including cancers. Because miRNAs are dysregulated in disease, miRNAs show promise as highly stable biomarkers. Formalin-fixed, paraffin-embedded (FFPE) tissue is a valuable sample type to assay for biomolecules because it is a convenient storage method and is often used by pathologists for histological staining. However, extracting biomolecules from FFPE tissue is challenging because of the presence of cellular and extracellular proteins, formaldehyde cross-links, and paraffin. Moreover, most protocols to measure miRNA in FFPE tissue are time-consuming and laborious. Here, we report a simple protocol to directly measure miRNA from formalin-fixed cells, FFPE tissue sections after paraffin is removed, and FFPE tissue sections using encoded hydrogel microparticles fabricated using stop flow lithography. Measurements by these particles show agreement between formalin-fixed cells and fresh cells, and measurement of FFPE tissue with paraffin is 10% less than FFPE tissue when paraffin is removed before the assay. When normal and tumor FFPE tissue are compared using this microparticle assay, we observe differential miRNA signal for oncogenic miRNAs and tumor suppressing miRNAs. This approach reduces assay times, reduces the use of hazardous chemicals to remove paraffin, and provides a sensitive, quantitative, and multiplexed measurement of miRNA in FFPE tissue.

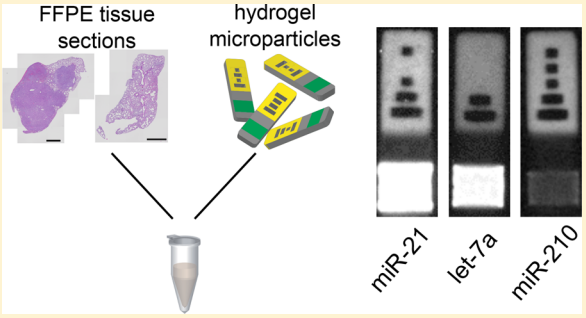

MicroRNAs (miRNAs) are small, noncoding RNAs[1] that are emerging as promising biomarkers because they have been shown to be dysregulated in many diseases, including cancers, and have high stability compared to other biomolecules.[2−5] However, quantifying miRNAs is challenging because miRNAs represent a small fraction (0.01%) of total RNA mass, their melting temperature varies with GC content, and different miRNAs can differ by single nucleotides.[6,7] Existing techniques, including quantitative reverse transcription polymerization chain reaction, DNA microarrays, and sequencing technologies, have high sensitivity, but they come up short in categories relevant to clinical diagnostic applications, such as multiplexing capacity, quantitation without sequence bias caused by target amplification, and/or assay duration.[6,8,9] Moreover, existing techniques often require the isolation of total RNA from a sample before measuring miRNA, involving time-consuming separation techniques.[6]

Formalin-fixed, paraffin-embedded (FFPE) tissue is a valuable sample type to assay for biomolecules because it is currently used by pathologists, it is a convenient storage method, it is possible to cut into thin sections, and there is the potential to assay samples from the same patient over time. Moreover, paraffin tissue blocks have been collected for more than a century and include many diseases.[10] However, it is difficult to extract mRNA from these specimens because formaldehyde cross-links mRNA to other biomolecules, leading to transcript fragmentation during tissue de-cross-linking.[10,11] MiRNA expression profiles from FFPE tissue closely correlate with matched frozen specimens, indicating that miRNA does not fragment during tissue de-cross-linking,[12−15] which has spurred interest in studying miRNA in FFPE tissue samples.[16−19] Still, extracting miRNAs from FFPE tissue is challenging because of the presence of cellular and extracellular proteins, formaldehyde cross-links, and paraffin, and most methods to detect miRNA in FFPE tissue involve a long workflow of first removing paraffin, second removing the formaldehyde cross-links, third isolating total RNA, and finally measuring miRNA expression levels.[14]

Polyethylene glycol (PEG) hydrogel microparticles have been used to measure biomolecules from complex samples

Received: May 4, 2018
Accepted: July 27, 2018
Published: August 14, 2018

DOI: 10.1021/acs.analchem.8b02010
Anal. Chem. 2018, 90, 10279−10285

from total tumor RNA,[20] human serum,[21] and raw cell lysate[22] with minimal sample prep in previous work. PEG hydrogels also provide a nonfouling scaffold for solution-like binding kinetics between the probe and target biomolecules.[23] We used stop flow lithography (SFL)[24] to polymerize individual PEG microparticles with a probe region to quantify a specific miRNA, a code region to identify which miRNA the particle is detecting, and internal negative control regions.[20−22,25] This barcode design allows for more than 1000 distinct codes, more than is needed for a particular diagnostic experiment. 12-Plex assays have been demonstrated in previous work, with all 12 different particle types included in the same tube with the sample.[20] Diagnostic potential for certain diseases has been shown using miRNA library sizes of 13,[26] 7,[27,28] 5,[29] and 3.[30] Thus, this platform is well-equipped to handle a sufficient amount of multiplexing for diagnostic uses.

In this paper, we use encoded hydrogel microparticles to quantify miRNA directly from several formalin-fixed samples: formalin-fixed cells, FFPE tissue with paraffin removed, and FFPE tissue. We show agreement between frozen and fixed cells, and we identify a 10% reduction in overall assay signal in FFPE tissue compared to the case when paraffin was removed before the assay. We also observe differential miRNA signal for oncogenic miRNAs and tumor suppressing miRNAs when comparing FFPE nonsmall cell lung cancer tissue and FFPE normal lung tissue. This approach fits into the pathologist's workflow because the same starting material for typical pathological stains can be used for this assay with no additional sample preparation.

EXPERIMENTAL SECTION

Particle Synthesis. Particles were synthesized using stop flow lithography, as previously described.[20,22,24,31] Four monomer streams were coflowed through a polydimethylsiloxane (PDMS) microchannel (height ≈ 40 μm) to generate particles with four regions: (1) a barcode region that was copolymerized with rhodamine acrylate for visualization of the particle barcode, (2) an inert region that acted as an internal negative control, (3) a probe region that contained a DNA probe complementary to a miRNA of interest, and (4) a second inert region. The monomer solutions contained polyethylene glycol diacrylate (PEG-DA), MW = 700 g/mol, as monomer, polyethylene glycol (PEG), MW = 200 g/mol, as porogen, Darocur 1173 as UV-activated photoinitiator, and 1×Tris-EDTA (1×TE) buffer. We flowed the monomer solution through the channel using compressed air, stopped the flow, and transmitted ultraviolet light (Thorlabs, 365 nm LED, 720 mW/cm^2, 100 ms exposure time) through a mylar photomask (Fineline, designed in AUTOCAD) placed in the field stop of the microscope and through a 20× objective. Code and inert regions of the particles were composed of 35% PEG-DA diluted 9:1 with either rhodamine acrylate or color dye for stream visualization, and the probe region of the particles was composed of 20% PEG-DA diluted 9:1 with DNA probe solution. The full compositions of the four monomer streams are shown in Table S1. After particles were formed, they were removed from the channel and washed in 1×TET (1×Tris-EDTA buffer with 0.05% Tween 20) three times. In each wash step, 500 μL of 1×TET is added, tubes are vortexed for five seconds and centrifuged for 20 s, and 500 μL of supernatant is removed.

$KMnO_4$ was added to 0.1 M Tris-HCl (pH 8.8) to make a 600 μM solution. Particles were oxidized by adding 1 mL of $KMnO_4$ solution to 100 μL of particles in 1×TET and vortexing for 2 min. Particles were then washed in 1×TET three times.

Cell Fixation. Human lung cancer cell line Calu-6 was cultured in Dulbecco's Modified Eagle Medium with 10% fetal bovine serum, 2 mM L-glutamine, and 1% penicillin−streptomycin. Single cells were frozen with dimethyl sulfoxide in complete culture medium. Cells were kept in liquid nitrogen for long-term storage and in a −80 °C freezer for short-term storage. Before use, cells were thawed in room temperature media. Cells were fixed in paraformaldehyde by suspending cells in 1 mL of 4% paraformaldehyde in 1×PBS for 20 min. Fixed cells were then washed in 1×PBS and stored at 4 °C.

Animal Studies. All research involving animals complied with protocols approved by the Beth Israel Deaconess Medical Center Institutional Animal Care and Use Committee. Female NU/J (Nude) immunodeficient mice (4−6 weeks old, Jackson Laboratory #002019) were used for subcutaneous injections. 100 000 A549 cells in serum-free medium and growth factor reduced Matrigel (Corning #354230) (1:1) were inoculated into the flank of nude mice. The xenograft tumor formation was monitored by calipers twice a week. The recipient mice were monitored and euthanized when the tumors reached 1 cm in diameter. The tumor tissues from four transplanted mice were isolated and were processed for paraffin block preparation. *K-ras*$^{LSL\text{-}G12D/+}$; *p53*$^{fl/fl}$ (KP) genetically engineered mouse model for nonsmall cell lung cancer was established at the Beth Israel Deaconess Medical Center as reported previously.[32] In the same mouse lung, the tumor nodules and the far normal lung tissues, which are 1 cm away from tumor margins, were isolated and were processed for paraffin block preparation.

FFPE Tissue Preparation and H&E Staining. All of the tissues at 5 × 5 mm (length × width) were fixed in 4% paraformaldehyde for 24−48 h. After fixation, the tissues were dehydrated with ethanol and xylene. Then, the tissues were embedded into paraffin blocks. Sections (5 μm) of paraffin-embedded tissue were cut and placed onto glass microscope slides (Gold Seal). For hematoxylin and eosin (H&E) staining, the sections were stained with Hematoxylin and Eosin Y (Vector), dehydrated, and then covered with mounting medium (Vector). The images were taken under a microscope (Olympus).

Tissue Handling. For some FFPE tissue experiments, paraffin was removed before the assay, similar to a commercial protocol.[33] Tissue sections were removed from a slide by scraping with a scalpel and placing in a tube with ethanol. A new scalpel edge was used for each tissue section. Tubes of ethanol and tissue were vortexed and centrifuged at 10.0 RCF (relative centrifugal force) for 2 min to prevent the tissue from sticking to the sides of the tube. Ethanol was removed from the tube, and 1 mL of xylene was added to each tube. Tubes were vortexed for 15 s, centrifuged for 2 min at 10.0 RCF, and then heated at 50 °C for 3 min to melt the paraffin. The tubes were then vortexed for 15 s and centrifuged for 2 min at 10.0 RCF. The xylene was then removed. The tubes were washed in ethanol twice by adding 1 mL of ethanol, vortexing for 15 s, and centrifuging for 2 min at 10.0 RCF. After supernatant ethanol was removed, the tubes were left out in a fume hood to dry for 1 h. In other tissue experiments, FFPE tissue was added directly to tubes without the need for ethanol or xylenes.

MiRNA Assay Protocol. The assay for miRNA quantification from cell lysate, fixed cells, and FFPE tissue is split into

DOI: 10.1021/acs.analchem.8b02010
Anal. Chem. 2018, 90, 10279−10285

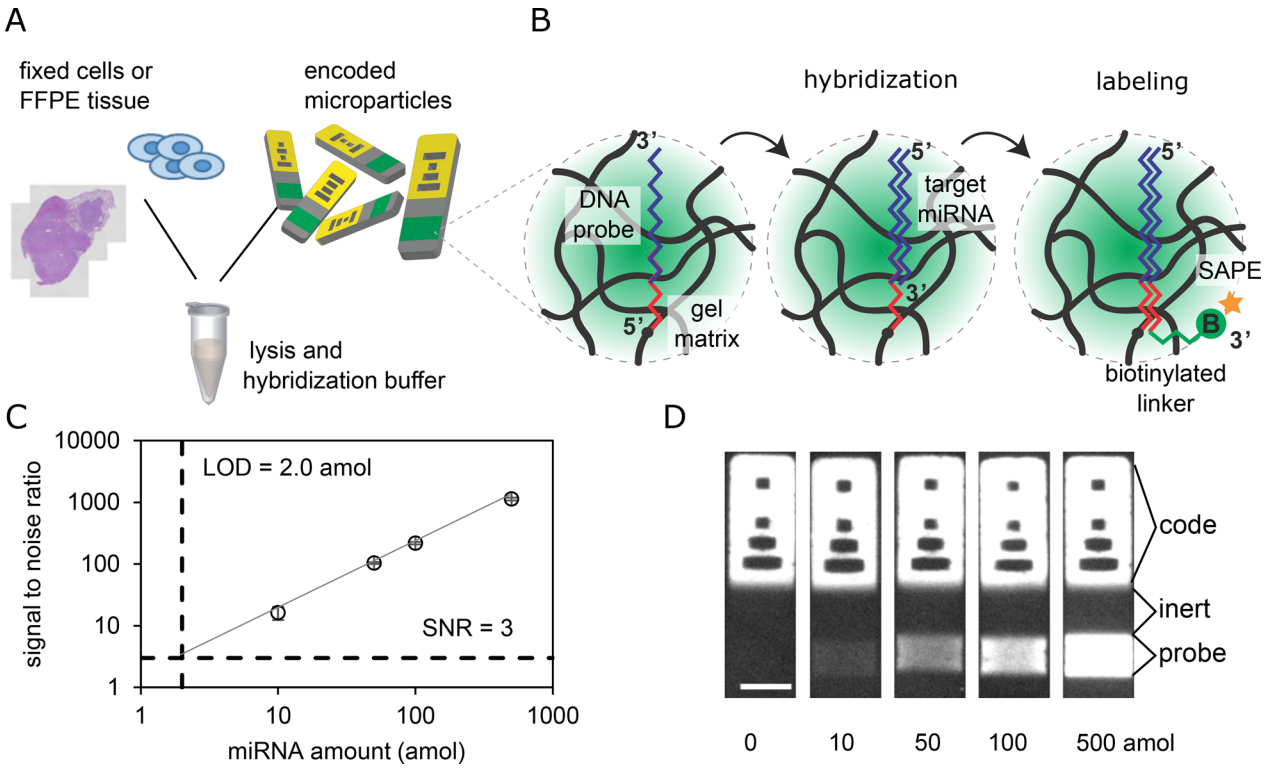

Figure 1. (A) miRNA-detecting hydrogel microparticles are added directly to fixed cells or the FFPE tissue section in experiments in this paper. (B) Target miRNA hybridizes to probes on the particles, the biotinylated adapter sequence is ligated to the end of the bound miRNA target, and streptavidin-R-phycoerythrin (SAPE) binds to biotin to allow fluorescence quantification. (C) Calibration curve for particles detecting miR-21, and (D) example particles from calibration curve. Scale bar = 50 μm. Limit of detection (LOD) is 2.0 amol. Error bars = 1 standard deviation.

four steps: (1) formalin cross-link degradation, (2) miRNA hybridization, (3) ligation, and (4) labeling (Figure 1A,B). (1) To remove the formalin cross-links, cells or tissue in 33 μL of 1×TET buffer containing 2% SDS and 8−32 U/mL proteinase K were heated at 50 °C for 15 min and 80 °C for 15 min (similar to a commercial protocol[33]) in a thermoshaker (MultiTherm Shaker, Thomas Scientific) at 1500 rpm. (2) As described previously,[20,22] particles were added, and the NaCl concentration was increased to 350 mM to promote DNA−miRNA hybridization in a volume of 50 μL. The samples were heated to 55 °C for 90 min at 1500 rpm. These salt and temperature conditions have been used previously to quantify many miRNAs.[20−22,34−36] Approximately 40 particles per miRNA target were added to each sample. While a larger sensing area may lead to a lower signal,[36,37] there needs to be enough particles to easily collect and analyze them at the end of the assay. Following the hybridization step, the particles were washed three times in wash buffer (50 mM NaCl in 1×TET) by adding 500 μL of wash buffer to 50 μL of solution, vortexing, centrifuging, and then removing 500 μL from the supernatant. These washing steps are done to dilute the hybridization solution contents by a factor of 1000. By doing so, we did not observe any proteinase K activity in remainder of the assay. (3) A ligation solution was prepared with 40 nM biotinylated linker sequence, 800 U/mL T4 DNA ligase, 250 μM ATP, 1×NEBuffer 2, and 1×TET. Ligation solution (235 μL) was added to the 50 μL particle solution and mixed in a thermoshaker for 30 min at 21.5 °C. During this step, the linker sequence hybridizes to the probe sequences and is ligated to miRNA bound to probe. Excess linker sequence is washed away during three wash steps in wash buffer. (4) In the labeling step, particles were incubated with 1.8 μg/mL streptavidin R-phycoerythrin (SAPE) in 1×TET and 50 mM NaCl for 45 min at 21.5 °C. After a final three wash steps in wash buffer, particles were imaged through a filter cube (Omega Optical XF101−2) on a Zeiss Axio Observer A1 microscope with a 20× objective, an Andor Clara CCD camera, and Andor SOLIS software. The standard deviation of an assay result was calculated using four to eight particles.

Image Analysis. Images were analyzed using ImageJ.[38] ImageJ was used to rotate particles and determine the average fluorescence intensity in the probe region of the particle. The net signal was calculated by subtracting the average fluorescence intensity in the probe region of a particle from the average fluorescence intensity in the probe region of negative control particles. As in prior work,[20,22] the limit of detection (LOD) was defined as the amount of miRNA required to generate a signal three times the standard deviation of the negative control when the signal-to-noise ratio (SNR) equals three. This was determined by generating a linear regression equation for log scaled data and finding the point where the signal was three times the standard deviation of the negative control. Using this approach, a lower limit of detection can be calculated in terms of the amount of miRNA and the number of cells.

RESULTS AND DISCUSSION

Evaluating Assay Performance with Synthetic miRNA. Assay performance of the hydrogel microparticles was determined by adding different amounts of synthetic miRNA to tubes containing miRNA-detecting hydrogel microparticles. MiRNA binds to DNA probes copolymerized

DOI: 10.1021/acs.analchem.8b02010
Anal. Chem. 2018, 90, 10279−10285

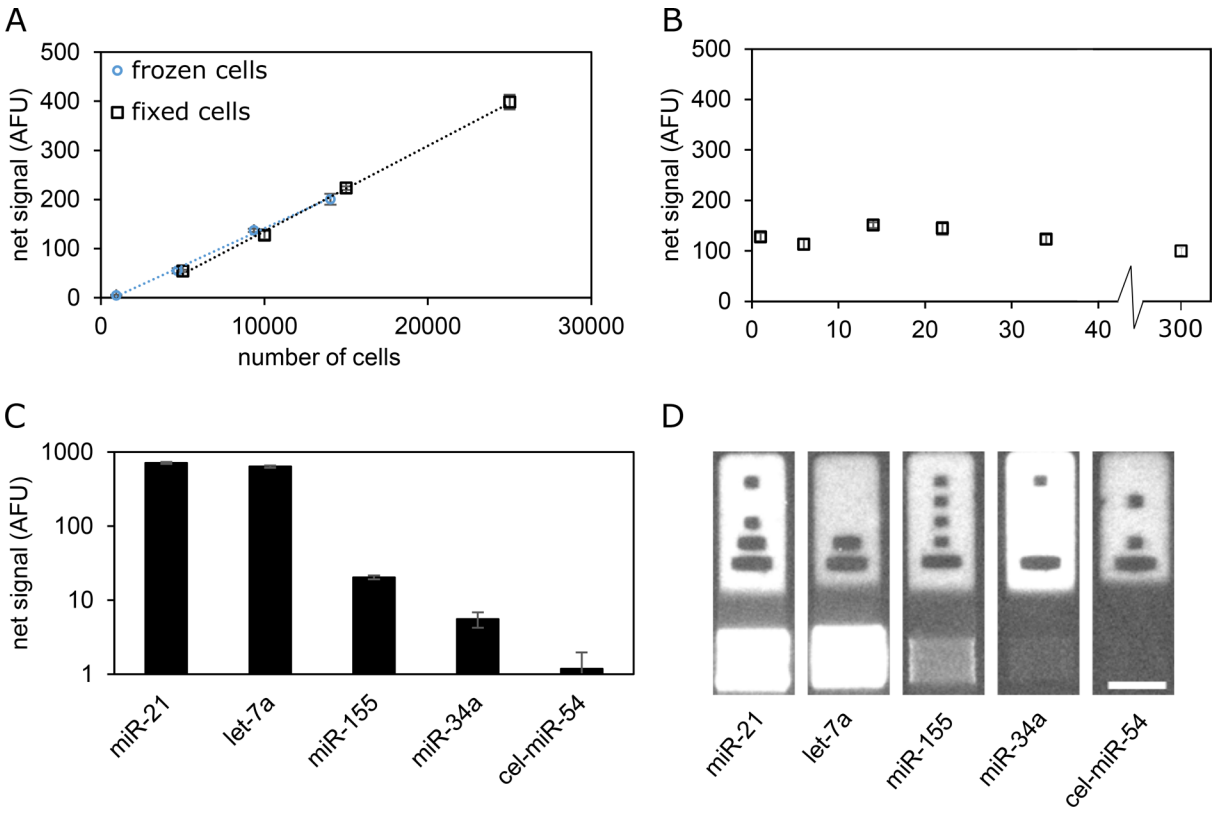

Figure 2. Multiplexed miRNA quantification from frozen and fixed Calu-6 cells. (A) miR-21 quantification from frozen and fixed Calu-6 cells. (B) miR-21 quantification from 10 000 fixed Calu-6 cells as a function of time after initial fixation. (C) Multiplexed quantification from 70 000 Calu-6 cells. (D) Representative particles of the five different miRNAs tested. Scale bar = 50 μm. Error bars = 1 standard deviation.

within the probe regions of the particles. Biotinylated linker and DNA ligase are added to attach a biotin to each location of miRNA binding. SAPE binds to the biotinylated linker and allows fluorescent quantification in the probe regions of the particles. These data were used to generate a calibration curve for miR-21, a highly expressed miRNA that has been linked to several cancers, including nonsmall cell lung cancer[39−41] (Figure 1C). The limit of detection (LOD) was determined by locating where the signal-to-noise ratio (SNR) equals three, which in this case is 2.0 amol. Example particles from the calibration curve assays are shown in Figure 1D. The limits of detection of other miRNAs used in this work are shown in Table S2.

Multiplexed miRNA Quantification from Frozen and Fixed Cells. Different from previous work with these hydrogel microparticles,[20,22] here the particles are first oxidized using $KMnO_4$, which was shown to reduce nonspecific binding of proteins to the particles by oxidizing unpolymerized double bonds.[34] We have found that oxidizing with $KMnO_4$ both increases the total assay signal in a cell assay and reduces nonspecific binding of cellular proteins to the hydrogel (Figure S1).

Before our goal of using the hydrogel microparticles to quantify miRNA in FFPE nonsmall cell lung cancer tissue, we first used hydrogel microparticles to quantify miRNA in Calu-6 cells, a nonsmall cell lung cancer cell line. Frozen Calu-6 cells were added directly to a tube with microparticles and lysis buffer to quantify miR-21 (Figure 2A). SDS and proteinase K were included in the hybridization buffer when quantifying miRNA from frozen cells to lyse membranes and degrade proteins complexed with miRNA as was done previously.[22] The limit of detection found here was approximately 700 cells, in close agreement with previous results of 850 NIH 3T3 cells measured in previous work.[22] We then fixed these cells in paraformaldehyde and stored them at 4 °C for up to 300 days. To quantify miRNA from formalin-fixed cells, SDS and proteinase K were added to the cells, and the mixture was heated to 50 °C for 15 min and 80 °C for 15 min to remove formaldehyde cross-links. We then added hybridization buffer and particles for miRNA quantification (Figures 2A,B). There is not a statistically significant difference between the miRNA signal measured per cell in fixed and frozen cells (P = 0.18) (Figure 2A), and the signal measured from 10 000 cells 300 days after fixation is only 15% less than the initial measurement (Figure 2B). These results indicate that the miRNA was well-preserved in the cells during the fixation step and well-preserved over time. Other recent work also shows that miRNA is well-preserved in and efficiently extracted from formalin-fixed cells and tissue.[11−15]

The barcodes on the hydrogel particles enable multiplexing. Using particles targeting two oncogenic miRNAs (miR-21 and miR-155),[40,42] two tumor suppressing miRNAs (let-7a and miR-34a),[2,43] and one control miRNA from *C. elegans* that has been previously used as a control (*cel*-miR-54),[22] we obtained a multiplexed measurement from Calu-6 cells (Figure 2C). Representative particles are shown in Figure 2D. The code regions of the particles in Figure 2D have different signal intensities because different amounts of rhodamine acrylate were in the monomer solutions during fabrication. The signal for *cel*-miR-54 was below the LOD of the assay.

Multiplexed miRNA Quantification from FFPE Tissue. After demonstrating miRNA quantification from fixed cells, we

DOI: 10.1021/acs.analchem.8b02010
Anal. Chem. 2018, 90, 10279−10285

used the encoded hydrogel microparticles to detect miRNA from FFPE tissue. We scraped FFPE tissue sections (~5 μm thick) off slides and placed them in tubes. In one experiment, tissue was washed in xylene to remove paraffin and heated with proteinase K and SDS as done for formalin-fixed cells, and then, particles were added to extract miRNA. In a second experiment, proteinase K and SDS were added directly to the FFPE tissue for formaldehyde cross-link removal, and then, particles were added to the sample containing paraffin (Figure 3). We found that the signal for miR-155 in these samples was below the limit of detection for the assay. We also added an additional target, miR-210, a marker for hypoxia in tissue.[44]

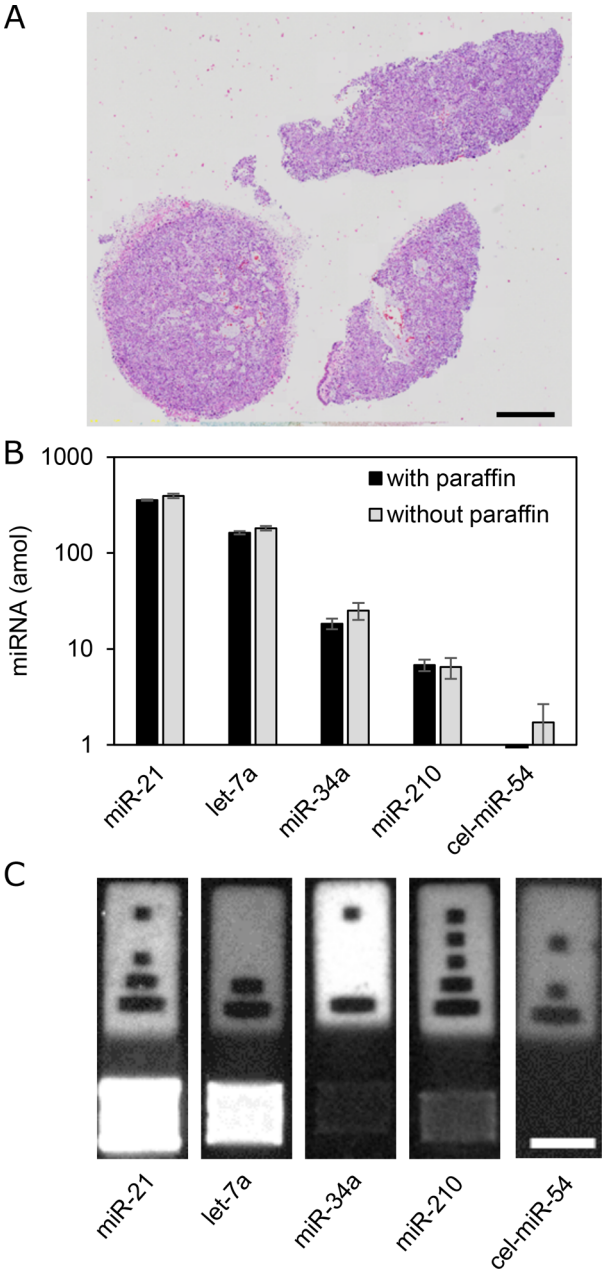

Figure 3. Multiplexed miRNA quantification from FFPE tissue with paraffin and after paraffin was removed. (A) H&E stain of proximal tissue section. Scale bar = 1 mm. (B) Results of quantification of 5 μm section with and without paraffin. (C) Representative particles from assay. Scale bar = 50 μm. Error bars = 1 standard deviation.

The signal from the particles with paraffin is only about 10% less than the signal from particles when paraffin was removed first. Over several separate experiments, this approach shows no more than 12% difference between a measurement with paraffin removed and one with paraffin (Figure S2). Some differences between samples are expected given biological variations between different sections of tissue. This demonstrates the utility of these nonfouling hydrogels for miRNA detection in FFPE tissue. Assaying the FFPE tissue directly is a substantial improvement over other methods of measuring miRNA from FFPE tissue, which generally involve removing paraffin, degrading the formaldehyde cross-links, separating nucleic acids, isolating total RNA, and finally measuring miRNA. Not only does this method save time and reduce the number of assay steps, this approach also removes the need for working with the hazardous chemical xylene to remove the paraffin.

Proteinase K was added to the hybridization step of the assay to degrade the formaldehyde cross-links by breaking up proteins inside the FFPE tissue. To optimize the assay with respect to the concentration of proteinase K, different concentrations of proteinase K were added to different tubes containing tissue sections, and the miR-21 signal was measured after completion of the miRNA assay (Figure 4). Synthetic *cel*-

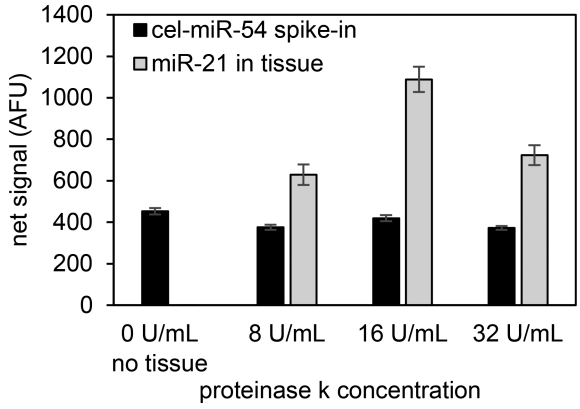

Figure 4. Optimization of proteinase K in tissue assay. Signal of miR-21 (present in tissue) shows the effects of proteinase K on amount of miRNA released from tissue and measured by microparticles, while signal of *cel*-miR-54 (not present in tissue) shows the effects of proteinase K and tissue on miRNA assay performance. Error bars = 1 standard deviation.

miR-54 was added as a positive control to determine if the presence of proteinase K and FFPE tissue affected the overall assay performance, independent of miRNA extraction efficiency or amount of miRNA in a tissue section. The signal from *cel*-miR-54 is about 15% less in the presence of tissue and proteinase K, further demonstrating small losses in the presence of paraffin and formaldehyde-cross-linked biomolecules. The 16 U/mL group has statistically significantly greater miR-21 signal than the 8 and 32 U/mL groups ($P < 0.001$ from a one-way analysis of variance followed by a Tukey honest significant difference test), and this increase in miR-21 signal is greater than the measured biological variations from proximal tissue sections (Figure S2).

We compared paired lung tissue sections from the same mouse in *K-ras*; *p53*-driven genetically engineered mouse models of nonsmall cell lung cancer. The tumor tissues from the tumor nodules form an adenocarcinoma-like structure with

DOI: 10.1021/acs.analchem.8b02010
Anal. Chem. 2018, 90, 10279−10285

a great degree of cellular pleomorphism and nuclear atypia, while the normal lung tissue, which is 1 cm away from the tumor margin, forms a normal alveoli structure with air sacs surrounded by alveolar epithelial cells (Figure 5A). To quantify miRNA from these samples, we placed five tissue sections of FFPE tumor tissue sections and 20 tissue sections of FFPE normal tissue sections into tubes to give roughly equal tissue volumes (the area of tissue on the normal tissue section was about 4 times smaller than the area of the tumor tissue section, see Figure S3). We normalized the assay results by tissue volume. We did not remove paraffin before the assay, noting that there is much more paraffin in these tubes than for the previous experiments, which had one section per tube. In tumor tissue, we observe greater expression of miR-21 ($P < 0.001$), an oncogenic miRNA in nonsmall cell lung cancer,[40] while in normal tissue, we observe greater expression of let-7a and miR-34a ($P < 0.001$), tumor suppressing miRNAs in nonsmall cell lung cancer (Figure 5B,C).[2,43] We do not observe a statistical difference between the two tissue types in terms of expression of miR-210, a marker for hypoxia.[44]

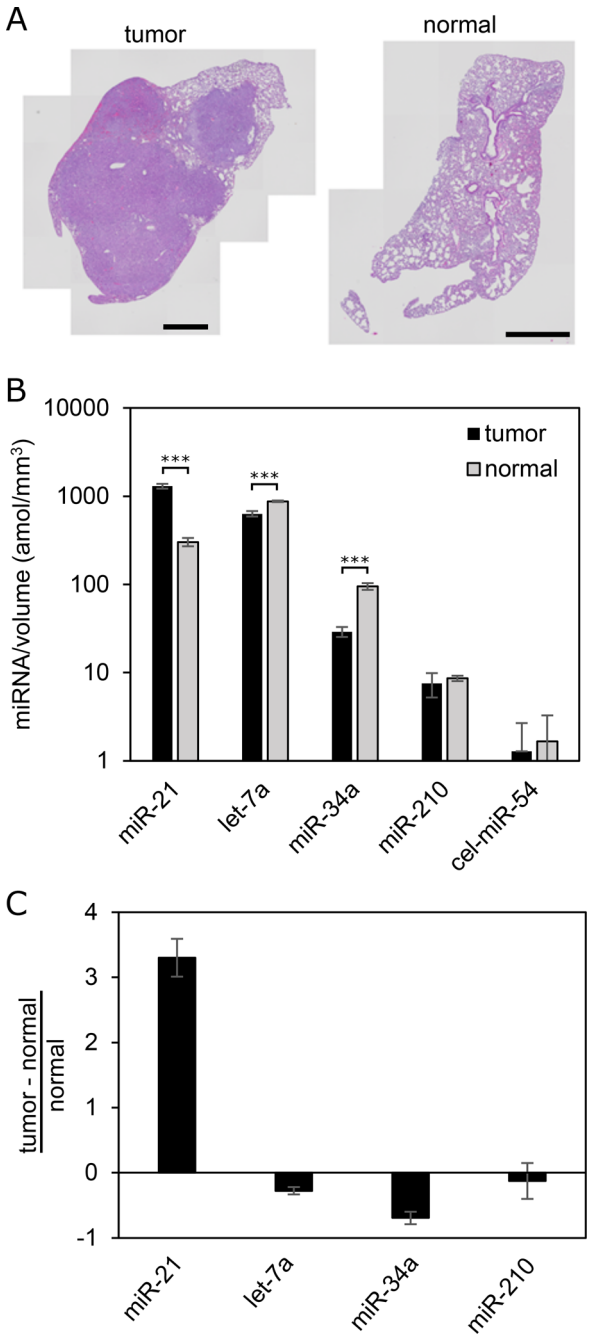

Figure 5. Comparison of normal and tumor tissue sections with multiplexed miRNA assay. (A) H&E stains of the paired tumor (left) and normal (right) tissue sections in the same mouse from the *K-ras*; *p53* genetically engineered mouse model of nonsmall cell lung cancer. Scale bars = 1 mm. (B) MiRNA signal normalized by volume of tissue for miR-21 (oncogenic miRNA[40]), let-7a and miR-34a (tumor suppressing miRNAs[2,43]), and miR-210 (hypoxia marker[44]). *** indicates $P < 0.001$ from two sample t test. (C) Normalized differential miRNA signal between tumor and normal tissue. *Cel*-miR-54 is quantified as a negative control. Error bars = 1 standard deviation.

CONCLUSIONS

Here we present a method to quantify miRNA directly from FFPE tissue using encoded hydrogel microparticles. The nonfouling nature of the hydrogels enables a direct measurement without the laborious sample prep required in other approaches. This approach also does not require the use of xylene, a hazardous chemical used to deparaffinize FFPE tissue. We envision this technology as an addition to the pathologist's toolbox, in that proximal tissue sections can be used for existing histological stains and quantitative miRNA assays.

ASSOCIATED CONTENT

Supporting Information

The Supporting Information is available free of charge on the ACS Publications website at DOI: 10.1021/acs.analchem.8b02010.

A list of reagents, additional supporting tables and figures, and a description of statistical methods are available as noted in the text (PDF)

AUTHOR INFORMATION

Corresponding Author

*E-mail pdoyle@mit.edu (P.S.D.)

ORCID

Maxwell B. Nagarajan: 0000-0003-3207-3282

Patrick S. Doyle: 0000-0003-2147-9172

Notes

The authors declare no competing financial interest.

ACKNOWLEDGMENTS

This work was supported by The Bridge Project, a partnership between the Koch Institute for Integrative Cancer Research at MIT and the Dana-Farber/Harvard Cancer Center, and partially by Cancer Center Support (core) Grant P30-CA14051 from the National Cancer Institute. The authors also gratefully acknowledge research funding support from an NIGMS/NIH Interdepartmental Biotechnology Training Program Fellowship (M.B.N.), a Ford Foundation Postdoctoral Fellowship (A.M.T.), a Ludwig Center Fund Postdoctoral Fellowship (A.M.T.), NIH-NRSA 5T32HL007893-20 (W.C.Z), the NIH-YALE SPORE in Lung Cancer P50CA196530-03S1 (F.J.S.), and NIH-NIBIB Grant 5R21EB024101-02 (P.S.D).

DOI: 10.1021/acs.analchem.8b02010
Anal. Chem. 2018, 90, 10279−10285

REFERENCES

(1) Bartel, D. P. *Cell* **2004**, *116*, 281−297.
(2) Esquela-Kerscher, A.; Slack, F. J. *Nat. Rev. Cancer* **2006**, *6* (4), 259−269.
(3) Calin, G. A.; Croce, C. M. *Nat. Rev. Cancer* **2006**, *6* (11), 857−866.
(4) Melo, S. A.; Esteller, M. *FEBS Lett.* **2011**, *585* (13), 2087−2099.
(5) Chen, P.-S.; Su, J.-L.; Hung, M.-C. *J. Biomed. Sci.* **2012**, *19* (1), 90.
(6) Pritchard, C. C.; Cheng, H. H.; Tewari, M. *Nat. Rev. Genet.* **2012**, *13* (5), 358−369.
(7) Baker, M. *Nat. Methods* **2010**, *7* (9), 687−692.
(8) Chugh, P.; Dittmer, D. P. *Wiley Interdiscip. Rev. RNA* **2012**, *3* (5), 601−616.
(9) Wang, B.; Howel, P.; Bruheim, S.; Ju, J.; Owen, L. B.; Fodstad, O.; Xi, Y. *PLoS One* **2011**, *6* (2), e17167.
(10) Lewis, F.; Maughan, N. J.; Smith, V.; Hillan, K.; Quirke, P. *J. Pathol.* **2001**, *195* (1), 66−71.
(11) Siebolts, U.; Varnholt, H.; Drebber, U.; Dienes, H.-P.; Wickenhauser, C.; Odenthal, M. *J. Clin. Pathol.* **2009**, *62* (1), 84−88.
(12) Li, J.; Smyth, P.; Flavin, R.; Cahill, S.; Denning, K.; Aherne, S.; Guenther, S. M.; O'Leary, J. J.; Sheils, O. *BMC Biotechnol.* **2007**, *7*, 36.
(13) Liu, A.; Tetzlaff, M. T.; Vanbelle, P.; Elder, D.; Feldman, M.; Tobias, J. W.; Sepulveda, A. R.; Xu, X. *Int. J. Clin. Exp. Pathol.* **2009**, *2* (6), 519−527.
(14) Doleshal, M.; Magotra, A. A.; Choudhury, B.; Cannon, B. D.; Labourier, E.; Szafranska, A. E. *J. Mol. Diagn.* **2008**, *10* (3), 203−211.
(15) Xi, Y.; Nakajima, G. O.; Gavin, E.; Morris, C. G.; Kudo, K.; Hayashi, K.; Ju, J. *RNA* **2007**, *13*, 1668−1674.
(16) Tetzlaff, M. T.; Liu, A.; Xu, X.; Master, S. R.; Baldwin, D. A.; Tobias, J. W.; Livolsi, V. A.; Baloch, Z. W. *Endocr. Pathol.* **2007**, *18* (3), 163−173.
(17) Chen, L.; Li, Y.; Fu, Y.; Peng, J.; Mo, M.-H.; Stamatakos, M.; Teal, C. B.; Brem, R. F.; Stojadinovic, A.; Grinkemeyer, M.; et al. *PLoS One* **2013**, *8* (1), e54213.
(18) Yan, L.-X.; Huang, X.-F.; Shao, Q.; Huang, M.-Y.; Deng, L.; Wu, Q.-L.; Zeng, Y.-X.; Shao, J.-Y. *RNA* **2008**, *14* (11), 2348−2360.
(19) Weng, L.; Wu, X.; Gao, H.; Mu, B.; Li, X.; Wang, J.-H.; Guo, C.; Jin, J. M.; Chen, Z.; Covarrubias, M. *J. Pathol.* **2010**, *222* (1), 41−51.
(20) Chapin, S. C.; Appleyard, D. C.; Pregibon, D. C.; Doyle, P. S. *Angew. Chem., Int. Ed.* **2011**, *50* (10), 2289−2293.
(21) Chapin, S. C.; Doyle, P. S. *Anal. Chem.* **2011**, *83* (18), 7179−7185.
(22) Lee, H.; Shapiro, S. J.; Chapin, S. C.; Doyle, P. S. *Anal. Chem.* **2016**, *88* (6), 3075−3081.
(23) Le Goff, G. C.; Srinivas, R. L.; Hill, W. A.; Doyle, P. S. *Eur. Polym. J.* **2015**, *72*, 386−412.
(24) Dendukuri, D.; Gu, S. S.; Pregibon, D. C.; Hatton, T. A.; Doyle, P. S. *Lab Chip* **2007**, *7* (7), 818−828.
(25) Srinivas, R. L.; Chapin, S. C.; Doyle, P. S. *Anal. Chem.* **2011**, *83*, 9138−9145.
(26) Montani, F.; Marzi, M. J.; Dezi, F.; Dama, E.; Carletti, R. M.; Bonizzi, G.; Bertolotti, R.; Bellomi, M.; Rampinelli, C.; Maisonneuve, P. *JNCI J. Natl. Cancer Inst.* **2015**, *107* (6), djv063.
(27) Zhou, J.; Yu, L.; Gao, X.; Hu, J.; Wang, J.; Dai, Z.; Wang, J.-F.; Zhang, Z.; Lu, S.; Huang, X.; et al. *J. Clin. Oncol.* **2011**, *29* (36), 4781−4788.
(28) Yu, L.; Todd, N. W.; Xing, L.; Xie, Y.; Zhang, H.; Liu, Z.; Fang, H.; Zhang, J.; Katz, R. L.; Jiang, F. *Int. J. Cancer* **2010**, *127* (12), 2870−2878.
(29) Chen, Z.-H.; Zhang, G.-L.; Li, H.-R.; Luo, J.-D.; Li, Z.-X.; Chen, G.-M.; Yang, J. *Prostate* **2012**, *72* (13), 1443−1452.
(30) Xing, L.; Todd, N. W.; Yu, L.; Fang, H.; Jiang, F. *Mod. Pathol.* **2010**, *23* (8), 1157−1164.
(31) Dendukuri, D.; Pregibon, D. C.; Collins, J.; Hatton, T. A.; Doyle, P. S. *Nat. Mater.* **2006**, *5* (5), 365−369.
(32) DuPage, M.; Dooley, A. L.; Jacks, T. *Nat. Protoc.* **2009**, *4* (7), 1064−1072.
(33) Life Technologies. RecoverAll™ Total Nucleic Acid Isolation Kit: Protocol; 2011.
(34) Lee, H.; Srinivas, R. L.; Gupta, A.; Doyle, P. S. *Angew. Chem., Int. Ed.* **2015**, *54* (8), 2477−2481.
(35) Kim, J. J.; Chen, L.; Doyle, P. S. *Lab Chip* **2017**, *17* (18), 3120−3128.
(36) Tentori, A. M.; Nagarajan, M. B.; Kim, J. J.; Zhang, W. C.; Slack, F. J.; Doyle, P. S. Quantitative and Multiplex microRNA Assays from Unprocessed Cells in Isolated Nanoliter Well Arrays. *Lab Chip* **2018**; Advance Article.
(37) Pregibon, D. C.; Doyle, P. S. *Anal. Chem.* **2009**, *81* (12), 4873−4881.
(38) Schneider, C. A.; Rasband, W. S.; Eliceiri, K. W. *Nat. Methods* **2012**, *9* (7), 671−675.
(39) Hatley, M. E.; Patrick, D. M.; Garcia, M. R.; Richardson, J. A.; Bassel-Duby, R.; van Rooij, E.; Olson, E. N. *Cancer Cell* **2010**, *18* (3), 282−293.
(40) Zhang, J.; Wang, J.; Zhao, F.; Liu, Q.; Jiang, K.; Yang, G. *Clin. Chim. Acta* **2010**, *411* (11−12), 846−852.
(41) Stenvold, H.; Donnem, T.; Andersen, S.; Al-Saad, S.; Valkov, A.; Pedersen, M. I.; Busund, L.-T.; Bremnes, R. M. *BMC Clin. Pathol.* **2014**, *14* (1), 9.
(42) Higgs, G.; Slack, F. *J. Clin. Bioinf.* **2013**, *3* (1), 17.
(43) Kasinski, A. L.; Slack, F. J. *Cancer Res.* **2012**, *72* (21), 5576−5587.
(44) Grosso, S.; Doyen, J.; Parks, S. K.; Bertero, T.; Paye, A.; Cardinaud, B.; Gounon, P.; Lacas-Gervais, S.; Noël, A.; Pouysségur, J.; et al. *Cell Death Dis.* **2013**, *4* (3), e544.

DOI: 10.1021/acs.analchem.8b02010
Anal. Chem. 2018, 90, 10279−10285